

High Affinity Glycodendrimers for the Lectin LecB from *Pseudomonas aeruginosa*

Nathalie Berthet,[†] Baptiste Thomas,[†] Isabelle Bossu,[†] Emilie Dufour,[†] Emilie Gillon,[‡] Julian Garcia,[†] Nicolas Spinelli,[†] Anne Imberty,[‡] Pascal Dumy,^{†,§} and Olivier Renaudet^{*,†,||}

[†]Département de Chimie Moléculaire, UMR-CNRS 5250 & ICMG FR 2607, Université Joseph Fourier, BP 53, 38041 Grenoble Cedex 9, France

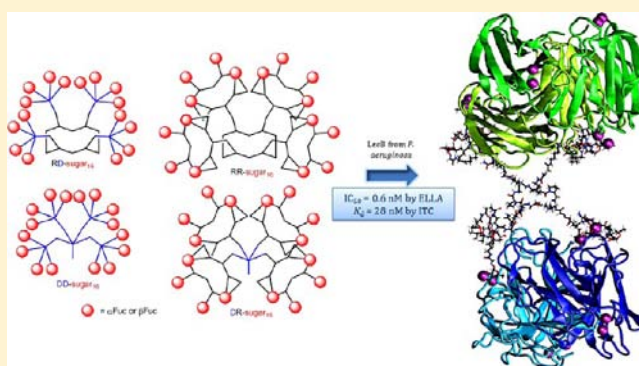
[‡]Centre de Recherche sur les Macromolécules Végétales (CERMAV – CNRS), affiliated with Université Joseph Fourier Grenoble and ICMG, BP 53, 38041 Grenoble, France

[§]Ecole Nationale Supérieure de Chimie de Montpellier, 8 Rue de l'École Normale, 34000 Montpellier, France

^{||}Institut Universitaire de France, 103 boulevard Saint-Michel, 75005 Paris, France

Supporting Information

ABSTRACT: Following an iterative oxime ligation procedure, cyclopeptide (R) and lysine-based dendron (D) were combined in all possible arrangements and successively functionalized with α -fucose and β -fucose to provide a new series of hexadecavalent glycosylated scaffolds (i.e., scaffolds RD₁₆, RR₁₆, DR₁₆, and DD₁₆). These compounds and smaller analogs (tetra- and hexavalent scaffolds R₄ and R₆) were used to evaluate the influence of the ligand valency and architecture, and of the anomer configuration in the binding to the α Fuc-specific lectin LecB from *Pseudomonas aeruginosa*. Competitive enzyme-linked lectin assays (ELLA) revealed that only the RD₁₆ architecture displaying α Fuc (**9A**) reaches strong binding improvement (IC₅₀ of 0.6 nM) over α MeFuc, and increases the α -selectivity of LecB. Dissociation constant of 28 nM was measured by isothermal titration calorimetry (ITC) for **9A**, which represents the highest affinity ligand ever reported for LecB. ITC and molecular modeling suggested that the high affinity observed might be due to an aggregative chelate binding involving four sugar head groups and two lectins. Interestingly, unprecedented binding effects were observed with β -fucosylated conjugates, albeit being less active than the corresponding ligands of the α Fuc series. In particular, the more flexible lysine-based dendritic structures (**15B** and **18B**) showed a slight inhibitory enhancement in comparison with those having cyclopeptide core.



INTRODUCTION

Carbohydrate–protein interactions fascinate glycoscientists because of their involvement in a variety of biological events including fertilization, cell–cell communication, cancer metastasis, immune response, and inflammation.^{1–4} Furthermore, bacterial or viral infections are initiated by highly specific multivalent recognition mechanisms between glycans displayed at the host cell surface and lectins expressed by these pathogens.^{5–7} *Pseudomonas aeruginosa* belongs to the bacteria that are being subjected to numbers of investigations. Isolated as antibiotic-resistant strains in hospital environment, this human opportunistic bacterium causes nosocomial infections and dramatic damages for immunocompromised patients.⁸ Notably, chronic colonization of lung with *P. aeruginosa* can be lethal for patients with cystic fibrosis. This bacterium produces two soluble tetrameric lectins (i.e., LecA and LecB specific for D-galactose and L-fucose, respectively) which were demonstrated to play crucial roles in diverse infection steps, going from the adhesion to host cells to the biofilm formation.⁹

Synthetic structures that could compete with natural ligands of these lectins can potentially prevent *P. aeruginosa* infection, therefore providing an ideal alternative to traditional antibiotic treatments.^{10–12}

Therapeutic effects observed recently with fucose and galactose^{13,14} are encouraging the development of higher-affinity ligands against *P. aeruginosa* that might be achieved by capitalizing on the well-known “glycoside cluster effect”.^{15–17} Although numbers of structures have been designed for the lectin LecA, only a few ligands have been reported so far for LecB. Biochemical and structural studies revealed that LecB is characterized by unusual micromolar affinity of LecB for fucose, which was attributed to the participation of two bridging calcium in the binding pocket and large enthalpy contribution.^{18–20} While higher affinities were observed with mono-

Received: May 14, 2013

Revised: July 23, 2013

Published: July 26, 2013

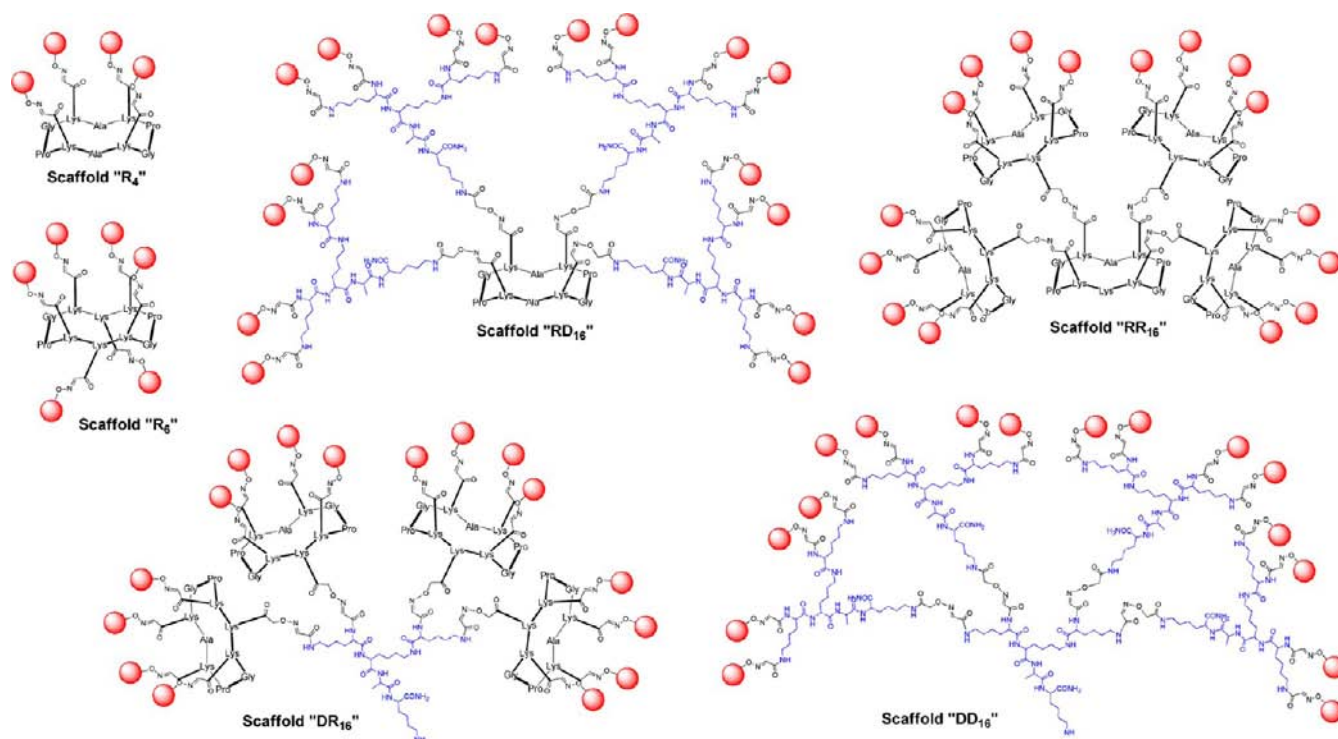


Figure 1. Structures of tetra- (R_4), hexa- (R_6), and hexadeca-valent (RD_{16} , RR_{16} , DR_{16} , DD_{16}) glycoclusters.

valent α -fucosylated oligosaccharides^{18–20} and glycomimetics,^{21,22} Roy et al. demonstrated by turbidimetric analysis that aromatic glycodendrimers displaying from 4 to 16 fucosides induce cross-linking of LecB.²³ Further studies with the α Fuc1–4GlcNAc epitope also revealed that the divalent cluster reaches high affinity (K_d of 90 nM) by a similar cross-linking process,^{21,24} while other multimeric presentations allow lower binding improvement.^{22,25} More remarkably, Reymond et al. have identified trivalent peptide dendrimers displaying C-linked fucoside from combinatorial libraries of neoglycopeptides varying in their architectures and the nature of the amino acids present in the branches. Their lead compound was found to both inhibit and disperse *P. aeruginosa* biofilm by combining multivalency effects with electrostatic interactions of the dendrimer arms with negatively charged residues near the fucose binding site.^{26–30} All these promising results convinced us to develop new multivalent glycoconjugates with the aim to discover higher affinity ligand for LecB. Thus we synthesized glycoclusters and glycodendrimers displaying both alpha or beta fucosides and we studied their binding properties toward the LecB lectin by competitive enzyme linked lectin assay (ELLA) and isothermal titration calorimetry (ITC).

Tetra-, hexa-, and hexadeca-valent scaffolds were selected in order to evaluate the influence of valency and architecture in the binding to LecB (Figure 1). RAFT (regioselectively addressable functionalized template) cyclopeptides^{31–34} containing four lysines oriented through the upper domain of the scaffold and two more lysines pointing on the other side were employed, affording tetra-valent (scaffold R_4)³⁵ and hexavalent (scaffold R_6) derivatives. Four different hexadeca-valent scaffolds were next prepared from the constrained RAFT cyclopeptide (R) and the flexible lysine-based dendron (D) that were conjugated in the all possible combinations. Cyclopeptide was first functionalized with the dendrimer (scaffold RD_{16}) or was self-condensed (scaffold RR_{16}) as reported previously.^{36,37} In

return, the lysine-based dendron was used as the core structure on which cyclopeptide (scaffold DR_{16}) and dendron (scaffold DD_{16}) were attached.

EXPERIMENTAL PROCEDURES

Materials. All chemical reagents were purchased from Aldrich (Saint-Quentin Fallavier, France) or Acros (Noisy-Le-Grand, France) and were used without further purification. All amino acids belong to the L-series. Protected amino acids and Fmoc-Gly-Sasrin resin were obtained from Advanced Chem-Tech Europe (Brussels, Belgium), Bachem Biochimie S.A.R.L. (Voisins-Les-Bretonneux, France), and France Biochem S.A. (Meudon, France). PyBOP was purchased from France Biochem. Reaction progress was monitored by reverse-phase HPLC on Waters equipment using C_{18} columns. Analytical and preparative separation was carried out at 1.0 mL/min (EC 125/3 nucleosil 300–5 C_{18}) and at 22 mL/min (VP 250/21 nucleosil 300–7 C_{18}) with UV monitoring at 214 and 250 nm using a linear A–B gradient (buffer A: 0.09% CF_3CO_2H in water; buffer B: 0.09% CF_3CO_2H in 90% acetonitrile). All cyclopeptide intermediates were analyzed by mass spectrometry using electrospray ionization on an Esquire 3000+ Bruker Daltonics in positive mode. 1H NMR and G-COSY were recorded in D_2O at 400 MHz with a Bruker Avance 400 spectrometer. Mass spectra for hexadeca-valent glycoclusters were performed on a MALDI-TOF AutoFlex I Bruker after sample pretreatment in an OligoR3 microcolumn (Applied Biosystems, USA) using 2,5-dihydroxybenzoic acid matrix. Bovine serum albumin (BSA) and SIGMA FAST O-phenylenediamine dihydrochloride (OPD) were purchased from Sigma-Aldrich. Polymeric α -L-fucopyranose (PAA- α Fuc) was obtained from Lectinity Holding, Inc., Moscow. Recombinant LecB was purified from *Escherichia coli* BL21(DE3) containing the plasmid pET25pa2l as described previously.³⁸

O- α -*L*-Fucopyranosylhydroxylamine (**A**). Compound **2** (520 mg, 1.20 mmol) was dissolved in methylhydrazine (3.1 mL, 60 mmol) and EtOH (3 mL). After stirring overnight at room temperature, the solvent was evaporated and the residue was recrystallized in absolute EtOH. Yield: 77% (165 mg); R_f = 0.15 (EtOH/CH₂Cl₂, 3/7); mp 164 °C; $[\alpha]_D$ -204.6 (c 1, H₂O); ¹H NMR (300 MHz, CD₃OD): δ 4.86 (d, 1H, $J_{1,2}$ = 4.4 Hz, H-1), 3.99 (bq, 1H, $J_{5,6}$ = 6.4 Hz, H-5), 3.76 (dd, 1H, $J_{3,4}$ = 4.0 Hz, $J_{3,2}$ = 10.0 Hz, H-3), 3.67–3.63 (m, 2H, H-2, H-4), 1.21 (d, 1H, $J_{5,6}$ = 6.4 Hz, CH₃); ¹³C NMR (75 MHz, D₂O): δ 104.9 (C-1), 74.5 (C-4), 72.4 (C-2), 70.5 (C-3), 68.5 (C-5), 17.4 (CH₃); ESI⁺-HRMS: m/z calcd for C₆H₁₄NO₅: 180.0871 [M+H]⁺; found: 180.0866.

O- β -*L*-Fucopyranosylhydroxylamine (**B**). Compound **B** was obtained from **3** (865 mg, 1.98 mmol) following the procedure described for compound **A**. Yield: 70% (248 mg); R_f = 0.15 (EtOH/CH₂Cl₂, 3/7); mp 170 °C; $[\alpha]_D$ +26.2 (c 1, H₂O); ¹H NMR (300 MHz, D₂O): δ 4.53 (d, 1H, $J_{1,2}$ = 8.1 Hz, H-1), 3.87 (bq, 1H, $J_{5,6}$ = 6.4 Hz, H-5), 3.81–3.79 (m, 1 H, H-4), 3.71 (dd, 1 H, $J_{3,4}$ = 3.3 Hz, $J_{2,3}$ = 9.6 Hz, H-3), 3.55 (dd, 1H, $J_{1,2}$ = 8.1 Hz, $J_{2,3}$ = 9.6 Hz, H-2), 1.33 (d, 3H, $J_{5,6}$ = 6.4 Hz, CH₃); ¹³C NMR (75 MHz, D₂O): δ 105.9 (C-1), 73.4 (C-3), 71.7 (C-4), 71.2 (C-5), 69.5 (C-2), 15.7 (CH₃); ESI⁺-HRMS: m/z calcd for C₆H₁₄NO₅: 180.0871 [M+H]⁺; found: 180.0875.

Tetravalent Glycoclusters (Scaffold R_d). Aldehyde-containing cyclopeptide **4** (5.0 mg, 4.2 μ mol) and aminoxy sugar **A** (6.1 mg, 33.8 μ mol) were dissolved in 0.1% TFA in water (10 mM). After 2 h stirring at 37 °C, the crude mixture was purified by preparative HPLC without additional treatment. α -fucosylated derivative **5A**: Yield: 66% (5.1 mg); analytical RP-HPLC: R_t = 7.8 min (C₁₈, 214 nm, 5–40% B in 15 min); ESI⁺-MS: m/z calcd for C₇₆H₁₂₃N₁₈O₃₄: 1831.8 [M+H]⁺; found: 1831.5. β -fucosylated derivative **5B** was obtained following the procedure described for **5A**: Yield: 65% (5.0 mg); analytical RP-HPLC: R_t = 7.4 min (C₁₈, 214 nm, 5–40% B in 15 min); ESI⁺-MS: m/z calcd for C₇₆H₁₂₂N₁₈O₃₄: 1876.8 [M+2Na]⁺; found: 1875.5.

Hexavalent Glycoclusters (Scaffold R_e). Aldehyde-containing cyclopeptide **6** (4.1 mg, 2.9 μ mol) and aminoxy sugar **A** (6.2 mg, 34.2 μ mol) were dissolved in 0.1% TFA in water (10 mM). After 2 h stirring at 37 °C, the crude mixture was purified by preparative HPLC without additional treatment. α -fucosylated derivative **7A**: Yield: 75% (5.1 mg); analytical RP-HPLC: R_t = 14.0 min (C₁₈, 214 nm, 5–40% B in 30 min); ESI⁺-MS: m/z calcd for C₉₈H₁₅₉N₂₂O₄₆: 2381.1 [M+H]⁺; found: 2381.2. β -fucosylated derivative **7B** was obtained following the procedure described for **7A**: Yield: 72% (5.0 mg); analytical RP-HPLC: R_t = 14.0 min (C₁₈, 214 nm, 5–40% B in 30 min); ESI⁺-MS: m/z calcd for C₉₈H₁₅₉N₂₂O₄₆: 2381.1 [M+H]⁺; found: 2381.2. β -galactosylated derivative **7C** was obtained following the procedure described for **7A**: Yield: 68% (5.0 mg); analytical RP-HPLC: R_t = 13.0 min (C₁₈, 214 nm, 5–40% B in 30 min); ESI⁺-MS: m/z calcd for C₉₈H₁₅₉N₂₂O₅₂: 2478.0 [M+H]⁺; found: 2478.3.

Hexadecavalent Glycoclusters (Scaffold RD_{1e}). Aldehyde-containing cyclopeptide **8** (5.3 mg, 1.1 μ mol) and aminoxy sugar **A** (6.4 mg, 35.8 μ mol) were dissolved in 0.1% TFA in water (10 mM). After 2 h stirring at 37 °C, the crude mixture was purified by preparative HPLC without additional treatment. α -fucosylated derivative **9A**: Yield: 65% (5.3 mg); analytical RP-HPLC: R_t = 13.0 min (C₁₈, 214 nm, 5–40% B in 30 min); ¹H NMR (400 MHz, D₂O): δ 7.83–7.77 (m, 20H, 20 \times H_{ox}), 5.15–5.12 (m, 16H, 16 \times H-1), 4.76–4.71 (m, 8H, 4 \times

CH₂O), 4.45–4.23 (m, 28H, 28 \times H_a), 4.12 (d, 2H, ² $J_{H\alpha,H\alpha'}$ = 17.8 Hz, 2 \times H _{α Gly}), 4.03–3.99 (m, 16H, 16 \times H-4), 3.89–3.70 (m, 86H, 16 \times H-2, 16 \times H-3, 16 \times H-5, 32 \times H-6, 2 \times H _{α Gly}, 2 \times CH_{2 δ Pro}), 3.35–3.20 (m, 40H, 20 \times CH_{2 ϵ Lys}), 2.35–1.32 (m, 146H); MALDI-TOF-MS: m/z calcd for C₂₉₆H₄₈₂NaN₇₄O₁₃₈: 7307.3 [M+Na]⁺; found: 7308.6. β -fucosylated derivative **9B** was obtained following the procedure described for **9A**: Yield: 70% (5.8 mg); analytical RP-HPLC: R_t = 15.9 min (C₁₈, 214 nm, 5–40% B in 30 min); MALDI-TOF-MS: m/z calcd for C₂₉₆H₄₈₃N₇₄O₁₃₈: 7287.3 [M+H]⁺; found: 7287.9; ¹H NMR (400 MHz, D₂O): δ 7.88–7.78 (m, 20H, 20 \times H_{ox}), 5.15–5.08 (m, 16H, 16 \times H-1), 4.76–4.71 (m, 8H, 4 \times CH₂O), 4.48–4.23 (m, 28H, 28 \times H_a), 4.16–4.13 (m, 2H, 2 \times H _{α Gly}), 4.00–3.74 (m, 86H, 16 \times H-3, 16 \times H-5, 32 \times H-6, 2 \times H _{α Gly}, 2 \times CH_{2 δ Pro}), 16 \times H-4, 3.35–3.20 (m, 56H, 16 \times H-2, 20 \times CH_{2 ϵ Lys}), 2.35–1.32 (m, 146H).

Hexadecavalent Glycoclusters (Scaffold RR_{1e}). Aldehyde-containing cyclopeptide **10** (4.9 mg, 0.8 μ mol) and aminoxy sugar **A** (4.4 mg, 24.4 μ mol) were dissolved in 0.1% TFA in water (10 mM). After 2 h stirring at 37 °C, the crude mixture was purified by preparative HPLC without additional treatment. α -fucosylated derivative **11A**: Yield: 89% (6.1 mg); analytical RP-HPLC: R_t : 5.7 min (C₁₈, 214 nm, 5–100% B in 15 min); ¹H NMR (400 MHz, D₂O): δ 7.84–7.66 (m, 20H, 20 \times H_{ox}), 5.08–4.97 (m, 16H, 16 \times H-1), 4.43–4.20 (m, 40H, 40 \times H_a), 4.06–3.56 (m, 110H, 16 \times H-2, 16 \times H-3, 16 \times H-4, 16 \times H-5, 10 \times H _{α Gly}, 20 \times CH_{2 δ Pro}), 3.38–3.10 (m, 48H, 24 \times CH_{2 ϵ Lys}), 3.04 (t, 2H, ³ $J_{He,H\delta}$ = 8.0 Hz, CH_{2 ϵ Lys}), 2.33–2.18 (m, 10H, 10 \times H _{β Pro}), 2.11–1.08 (m, 253H); MALDI-TOF-MS: m/z calcd for C₃₇₉H₆₀₆N₉₅O₁₅₈: 9021.2 [M+H]⁺; found: 9022.2. β -fucosylated derivative **11B** was obtained following the procedure described for **11A**: Yield: 88% (6.0 mg); analytical RP-HPLC: R_t : 5.7 min (C₁₈, 214 nm, 5–100% B in 15 min); ¹H NMR (400 MHz, D₂O): δ 7.84–7.66 (m, 20H, 20 \times H_{ox}), 5.08–4.97 (m, 16H, 16 \times H-1), 4.43–4.20 (m, 40H, 40 \times H_a), 4.11–3.98 (m, 16H, 16 \times H-3), 3.89–3.80 (m, 16H, 16 \times H-5), 3.77–3.56 (m, 62H, 16 \times H-2, 16 \times H-4, 10 \times H _{α Gly}, 20 \times CH_{2 δ Pro}), 3.38–3.10 (m, 48H, 24 \times CH_{2 ϵ Lys}), 3.04 (t, 2H, ³ $J_{He,H\delta}$ = 8.0 Hz, CH_{2 ϵ Lys}), 2.33–2.18 (m, 10H, 10 \times H _{β Pro}), 2.11–1.08 (m, 253H); MALDI-TOF-MS: m/z calcd for C₃₇₉H₆₀₆N₉₅O₁₅₈: 9021.2 [M+H]⁺; found: 9021.6.

Aldehyde-Containing Scaffold (14). Aldehyde-containing dendrimer **12** (3.1 mg, 3.9 μ mol) and cyclopeptide **13** (44.4 mg, 30.1 μ mol) were dissolved in 0.1% TFA in water (10 mM). Complete conversion was observed by analytical HPLC after 2 h at 37 °C to provide scaffold DR_{1e}Ser. Analytical RP-HPLC: R_t : 8.5 min (C₁₈, 214 nm, 5–60% B in 20 min); ESI⁺-MS: m/z calcd for C₂₇₉H₄₈₁N₉₀O₈₉: 6519.6 [M+H]⁺; found: 6519.4. Acetone (100 μ L) was added to the crude mixture to quench the excess of **13** followed by sodium periodate (131 mg, 0.6 mmol). The crude mixture was stirred at room temperature 30 min and was finally purified by semipreparative HPLC. Yield: 78% (18 mg); analytical RP-HPLC: R_t = 9.8 min (C₁₈, 214 nm, 5–60% B in 20 min); ¹H NMR (400 MHz, D₂O): δ 7.84 (s, 2H, 2 \times H_{ox}), 7.78 (s, 2H, 2 \times H_{ox}), 5.34–5.30 (s, 8H, 8 \times CH(OH)₂), 4.52–4.12 (m, 45H, 4 \times CH₂O, 5 \times H _{α Lys}, 19 \times H _{α Lys}, 5 \times H _{α Alav}, 8 \times H _{α Pro}), 3.93–3.66 (m, 24H, 8 \times H _{α Gly}, 16 \times H _{δ Pro}), 3.36–3.17 (m, 46H, 23 \times H _{ϵ Lys}), 3.06–3.02 (m, 2H, 2 \times H _{ϵ Lys}), 2.42–1.25 (m, 191H).

Hexadecavalent Glycoclusters (Scaffold DR_{1e}). Aldehyde-containing cyclopeptide **14** (5.3 mg, 0.9 μ mol) and aminoxy sugar **A** (5.1 mg, 28.2 μ mol) were dissolved in 0.1% TFA in water (10 mM). After 2 h stirring at 37 °C, the crude mixture

was purified by preparative HPLC without additional treatment. α -fucosylated derivative **15A**: Yield: 66% (5.0 mg); analytical RP-HPLC: R_t : 10.8 min (C_{18} , 214 nm, 5–60% B in 20 min); $^1\text{H NMR}$ (400 MHz, D_2O): δ 7.83–7.66 (m, 20H, 20 \times H_{ox}), 5.82–5.48 (m, 16H, 16 \times H-1), 4.64–4.47 (m, 13H, 4 \times CH_2O , 5 \times $\text{H}_{\alpha\text{Lys}}$), 4.41–4.18 (m, 32H, 19 \times $\text{H}_{\alpha\text{Lys}}$, 5 \times $\text{H}_{\alpha\text{Ala}}$, 8 \times $\text{H}_{\alpha\text{Pro}}$), 4.12–3.01 (m, 24H, 8 \times $\text{H}_{\alpha\text{Gly}}$, 16 \times H-5), 3.85–3.54 (m, 64H, 16 \times H-2, 16 \times H-3, 16 \times H-4, 16 \times $\text{H}_{\delta\text{Pro}}$), 3.34–3.10 (m, 46H, 23 \times H_{eLys}), 2.98–2.92 (m, 2H, 2 \times H_{eLys}), 2.32–2.20 (m, 8H, 8 \times $\text{H}_{\beta\text{Pro}}$), 2.07–1.23 (m, 183H), 1.19–1.09 (m, 48H, 16 \times CH_3Fuc); MALDI-TOF-MS: m/z calcd for $\text{C}_{359}\text{H}_{577}\text{N}_{90}\text{O}_{153}$: 8603.0 $[\text{M}+\text{H}]^+$; found: 8606.6. β -fucosylated derivative **15B** was obtained following the procedure described for **15A**: Yield: 75% (5.6 mg); analytical RP-HPLC: R_t : 10.8 min (C_{18} , 214 nm, 5–60% B in 20 min); $^1\text{H NMR}$ (400 MHz, D_2O): δ 7.83–7.66 (m, 20H, 20 \times H_{ox}), 5.82–5.48 (m, 16H, 16H-1), 4.64–4.47 (m, 13H, 4 \times CH_2O , 5 \times $\text{H}_{\alpha\text{Lys}}$), 4.41–4.18 (m, 32H, 19 \times $\text{H}_{\alpha\text{Lys}}$, 5 \times $\text{H}_{\alpha\text{Ala}}$, 8 \times $\text{H}_{\alpha\text{Pro}}$), 4.12–3.01 (d, 8H, $^2J_{\text{H}\alpha,\text{H}\alpha'} = 17.1$ Hz, 8 \times $\text{H}_{\alpha\text{Gly}}$), 3.92–3.54 (m, 80H, 16 \times H-2, 16 \times H-3, 16 \times H-4, 16 \times H-5, 16 \times $\text{H}_{\delta\text{Pro}}$), 3.34–3.10 (m, 46H, 23 \times H_{eLys}), 2.98–2.92 (m, 2H, 2 \times H_{eLys}), 2.32–2.20 (m, 8H, 8 \times $\text{H}_{\beta\text{Pro}}$), 2.14–1.09 (m, 231H); MALDI-TOF-MS: m/z calcd for $\text{C}_{359}\text{H}_{577}\text{N}_{90}\text{O}_{153}$: 8603.0 $[\text{M}+\text{H}]^+$; found: 8599.6. β -galactosylated derivative **15C** was obtained following the procedure described for **15A**: Yield: 73% (5.4 mg); analytical RP-HPLC: R_t : 10.0 min (C_{18} , 214 nm, 5–60% B in 20 min); $^1\text{H NMR}$ (400 MHz, D_2O): δ 7.80–7.66 (m, 20H, 20 \times H_{ox}), 5.01–4.99 (m, 16H, 16 \times H-1), 4.64–4.47 (m, 13H, 4 \times CH_2O , 5 \times $\text{H}_{\alpha\text{Lys}}$), 4.39–4.14 (m, 32H, 19 \times $\text{H}_{\alpha\text{Lys}}$, 5 \times $\text{H}_{\alpha\text{Ala}}$, 8 \times $\text{H}_{\alpha\text{Pro}}$), 3.91–3.82 (d, 8H, $^2J_{\text{H}\alpha,\text{H}\alpha'} = 17.1$ Hz, 8 \times $\text{H}_{\alpha\text{Gly}}$), 3.94 (m, 16H, 16 \times H-4), 3.85–3.54 (m, 96H, 16 \times H-3, 16 \times H-2, 16 \times H-5, 32 \times H-6, 16 \times $\text{H}_{\delta\text{Pro}}$), 3.29–3.12 (m, 46H, 23 \times H_{eLys}), 2.98–2.92 (m, 2H, 2 \times H_{eLys}), 2.37–2.20 (m, 8H, 8 \times $\text{H}_{\beta\text{Pro}}$), 2.12–1.17 (m, 183H); MALDI-TOF-MS: m/z calcd for $\text{C}_{359}\text{H}_{577}\text{N}_{90}\text{O}_{169}$: 8858.0 $[\text{M}+\text{H}]^+$; found: 8859.0.

Aldehyde-Containing Scaffold (17). Aldehyde-containing scaffold **17** was obtained from **12** (3.4 mg, 4.1 μmol) and **16** (33.5 mg, 32.8 μmol) following the procedure described for **14**. Scaffold DD_{16}Ser : ESI⁺-MS: m/z calcd for $\text{C}_{199}\text{H}_{365}\text{N}_{70}\text{O}_{69}$: 4841.7 $[\text{M}+\text{H}]^+$; found: 4841.6. Scaffold **17**: Yield: 63% (3.5 mg); analytical RP-HPLC: R_t : 9.0 min (C_{18} , 214 nm, 5–60% B in 20 min); $^1\text{H NMR}$ (400 MHz, D_2O): δ 7.86 (s, 2H, 2 \times H_{ox}), 7.79 (s, 2H, 2 \times H_{ox}), 5.38 (s, 8H, 8 \times $\text{CH}(\text{OH})_2$), 5.32 (s, 8H, 8 \times $\text{CH}(\text{OH})_2$), 4.40–4.25 (m, 29H, 20 \times $\text{H}_{\alpha\text{Lys}}$, 5 \times $\text{H}_{\alpha\text{Ala}}$, 4 \times CH_2O), 3.36–3.16 (m, 38H, 19 \times H_{eLys}), 3.02–2.98 (m, 2H, 2 \times H_{eLys}), 1.92–1.30 (m, 135H).

Hexadecavalent Glycoclusters (Scaffold DD_{16}). Aldehyde-containing cyclopeptide **17** (3.1 mg, 0.7 μmol) and aminoxy sugar **A** (4.4 mg, 24.6 μmol) were dissolved in 0.1% TFA in water (10 mM). After 2 h stirring at 37 $^\circ\text{C}$, the crude mixture was purified by preparative HPLC without additional treatment. α -fucosylated derivative **18A**: Yield: 73% (3.9 mg); analytical RP-HPLC: R_t : 10.0 min (C_{18} , 214 nm, 5–60% B in 20 min); $^1\text{H NMR}$ (400 MHz, D_2O): δ 7.77 (s, 10H, 10 \times H_{ox}), 7.72 (s, 8H, 8 \times H_{ox}), 7.69 (s, 2H, 2 \times H_{ox}), 5.58–5.50 (m, 16H, 16 \times H-1), 4.39–4.15 (m, 33H, 20 \times $\text{H}_{\alpha\text{Lys}}$, 5 \times $\text{H}_{\alpha\text{Ala}}$, 4 \times CH_2O), 4.04 (m, 16H, 16 \times H-5), 3.98–3.76 (m, 48H, 16 \times H-2, 16 \times H-3, 16 \times H-4), 3.29–3.10 (m, 38H, 19 \times H_{eLys}), 2.98–2.92 (m, 2H, 2 \times H_{eLys}), 1.87–1.21 (m, 183H); MALDI-TOF-MS: m/z calcd for $\text{C}_{279}\text{H}_{461}\text{N}_{70}\text{O}_{133}$: 6923.1 $[\text{M}+\text{H}]^+$; found: 6924.4. β -fucosylated derivative **18B** was obtained following the procedure described for **18A**: Yield: 70% (1.8

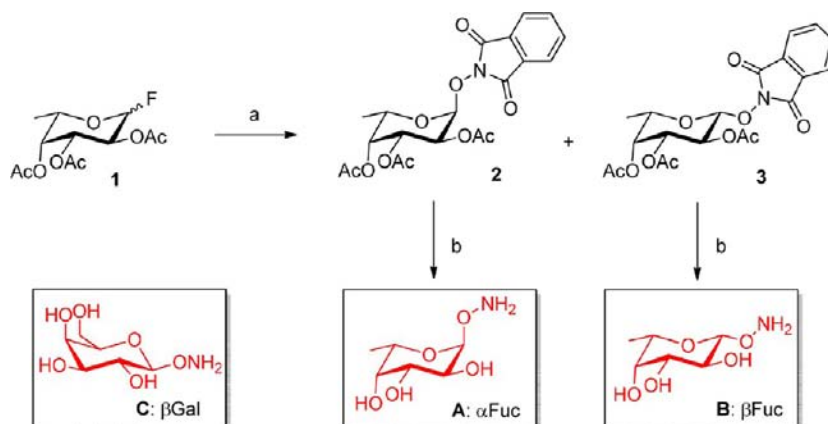
mg); analytical RP-HPLC: R_t : 10.0 min (C_{18} , 214 nm, 5–60% B in 20 min); $^1\text{H NMR}$ (400 MHz, D_2O): δ 7.82–7.66 (m, 20H, 20 \times H_{ox}), 5.03 (m, 16H, 16 \times H-1), 4.39–4.14 (m, 33H, 20 \times $\text{H}_{\alpha\text{Lys}}$, 5 \times $\text{H}_{\alpha\text{Ala}}$, 4 \times CH_2O), 3.91–3.82 (m, 16H, 16 \times H-5), 3.77–3.65 (m, 48H, 16 \times H-2, 16 \times H-3, 16 \times H-4), 3.29–3.12 (m, 38H, 19 \times H_{eLys}), 2.98–2.92 (m, 2H, 2 \times H_{eLys}), 1.87–1.21 (m, 183H); MALDI-TOF-MS: m/z calcd for $\text{C}_{279}\text{H}_{461}\text{N}_{70}\text{O}_{133}$: 6923.1 $[\text{M}+\text{H}]^+$; found: 6922.8. β -galactosylated derivative **18C** was obtained following the procedure described for **18A**: Yield: 65% (3.4 mg); analytical RP-HPLC: R_t : 9.5 min (C_{18} , 214 nm, 5–100% B in 20 min); $^1\text{H NMR}$ (400 MHz, D_2O): δ 7.81 (s, 8H, 8 \times H_{ox}), 7.75 (s, 9H, 9 \times H_{ox}), 7.70 (s, 3H, 3 \times H_{ox}), 5.06 (m, 16H, 16 \times H-1), 4.39–4.14 (m, 33H, 20 \times $\text{H}_{\alpha\text{Lys}}$, 5 \times $\text{H}_{\alpha\text{Ala}}$, 4 \times CH_2O), 3.94 (s, 16H, 16 \times H-4), 3.83–3.65 (m, 80H, 16 \times H-2, 16 \times H-3, 16 \times H-5, 32 \times H-6), 3.29–3.09 (m, 38H, 19 \times H_{eLys}), 2.98–2.92 (m, 2H, 2 \times H_{eLys}), 1.87–1.21 (m, 135H); MALDI-TOF-MS: m/z calcd for $\text{C}_{279}\text{H}_{461}\text{N}_{70}\text{O}_{149}$: 7182.1 $[\text{M}+\text{H}]^+$; found: 7183.0.

Enzyme-Linked Lectin Assays. LecB (2 mg) dissolved in PBS was incubated for 2 h at room temperature with 10 mM of biotinamidohexanoyl-6-aminohexanoic acid *N*-hydroxysuccinimide ester diluted in DMF. At the end of the incubation, unreacted biotinylation reagent was removed by dialysis and the lectin was lyophilized. ELLA experiments were conducted using 96-well microtiter Nunc-Immuno plates (Maxi-Sorp) coated with PAA- α -L-fucose (5 $\mu\text{g}\cdot\text{mL}^{-1}$) diluted in carbonate buffer pH 9.6 (100 μL) for 1 h at 37 $^\circ\text{C}$. After removal of excess polymeric sugar, the wells were blocked with BSA in PBS (3% w/v, 100 μL per well) at 37 $^\circ\text{C}$ for 1 h. BSA solution was removed and each inhibitors was added in 2-fold serial dilution (50 μL per well) in PBS to PAA-sugar-coated microplates. Then 100 μL of biotinylated LecB (0.1 $\mu\text{g}\cdot\text{mL}^{-1}$) was added to the above solutions of inhibitors and the plate were incubated at 37 $^\circ\text{C}$ for 1 h. After washing with T-PBS (PBS + 0.05% Tween, 3 \times 100 $\mu\text{L}\cdot\text{well}^{-1}$) 100 μL of streptavidin–peroxidase conjugate (dilution 1:5000 in PBS + 3% BSA w/v) was added and left for 1 h at 37 $^\circ\text{C}$. The wells were washed with T-PBS (3 \times 100 $\mu\text{L}\cdot\text{well}^{-1}$), then the color was developed using 100 μL per well of 0.05 M phosphate/citrate buffer containing OPD (0.4 $\text{mg}\cdot\text{mL}^{-1}$) and urea hydrogen peroxide (0.4 $\text{mg}\cdot\text{mL}^{-1}$). The reaction was stopped after 10 min by the addition of 50 μL of 30% aqueous H_2SO_4 . The absorbance was read at 490 nm using a microtiter plate reader. The percentage of inhibition was plotted against the logarithm of the concentration of the sugar derivatives. The sigmoidal curve was fitted and the concentration at 50% inhibition of binding of the biotinylated LecB to PAA- α Fuc coated microtiter plates was determined. The percentage of inhibition were calculated as given in eq 1, where A = absorbance.

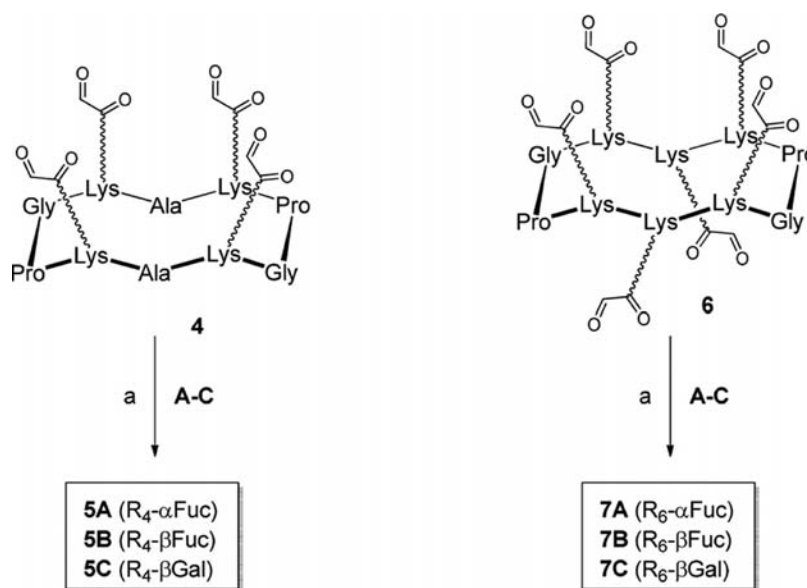
$$\% \text{inhibition} = \left[\frac{(A_{(\text{no inhibitor})} - A_{(\text{with inhibitor})})}{A_{(\text{no inhibitor})}} \right] \times 100 \quad (1)$$

The IC_{50} values were systematically performed in triplicate.

Isothermal Titration Calorimetry. ITC experiments were performed with a VP-ITC isothermal titration calorimeter (Microcal). The experiments were carried out at 25 $^\circ\text{C}$. Glycoconjugates **9A**, **9B**, and **15B** and LecB were dissolved in the same buffer composed of 20 mM Tris with 100 mM NaCl and 0.1 mM CaCl_2 at pH 7.5. The glycoclusters were placed in the microcalorimeter cell (1.447 mL) at concentrations varying from 2.5 to 4 μM . A total of 30 injections of 10 μL of LecB at concentrations varying from 0.23 to 0.25 mM were added at

Scheme 1. Synthesis of Aminoxy Glycosides A–C^a

^aReagents and conditions: (a) *N*-hydroxyphthalimide, $\text{BF}_3 \cdot \text{Et}_2\text{O}$, triethylamine, CH_2Cl_2 , rt, 4 h, 85% (α/β , 1/1.4); (b) methylhydrazine, EtOH (1/1, v/v), rt, 6 h, 77% for A, 70% for B.

Scheme 2. Synthesis of the Tetravalent (R_4) and Hexavalent (R_6) Glycoclusters^a

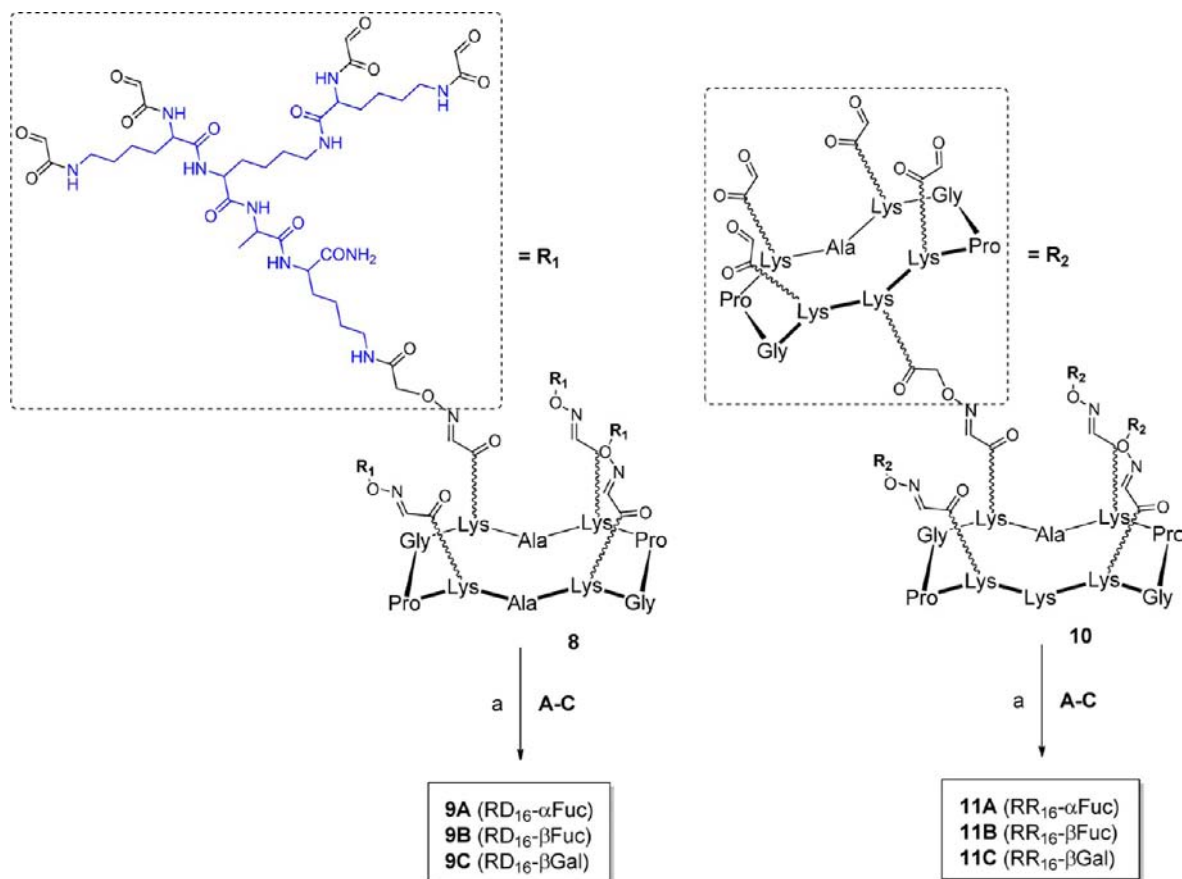
^aReagents and conditions: (a) 0.1% TFA in H_2O , 37 °C, 2 h, 66% for 5A; 65% for 5B; 74%⁴⁷ for 5C; 75% for 7A; 72% for 7B; 68% for 7C. All amino acids belong to the L-series.

intervals of 3.5 or 5 min while stirring at 310 rpm. Control experiments performed by injection of buffer into the protein solution yielded insignificant heats of dilution. The experimental data were fitted to a theoretical titration curve using Origin software supplied by Microcal, with ΔH (enthalpy change), K_a (association constant), and N (number of binding sites per monomer) as adjustable parameters. Dissociation constant (K_d), free energy change (ΔG), and entropy contributions ($T\Delta S$) were derived from the previous ones. Two or three independent titrations were performed for each ligand tested.

NMR Spectroscopy. NMR spectra were obtained at 500 MHz and 25 °C with a Bruker Avance spectrometer on 2–3 mM protein samples dissolved in $\text{H}_2\text{O}/\text{D}_2\text{O}$ (95:5). A number of two-dimensional TOCSY,³⁹ DQF-COSY,⁴⁰ and NOESY⁴¹ spectra were acquired with 1.5 s steady state recovery time, mixing times (tm) of 60 ms for TOCSY and 50–200 ms for NOESY. The spin-lock mixing of the TOCSY experiment was

obtained with a DIPSI-2⁴² pulse train at $\gamma B_2/2\pi = 9\text{--}10$ kHz. The acquisitions were performed over a spectral width of 5000 Hz in both dimensions, with matrix size of 2048 points in t_2 and 256–512 points in t_1 and 32–128 scans each t_1 free induction decay (FID). The water resonance was suppressed by adding an excitation-sculpting module⁴³ to the nonselective detection pulse and with selective Gaussian shaped pulses of 3–5 ms. Data processing and analysis were performed using Felix (Accelrys, San Diego, CA) software with shifted (60–90°) square sinebell window function prior to Fourier transformation and zero-filled in t_1 .

Distance Restraints and Molecular Modeling. Internuclear distances of compound 9A were quantified from the NOESY cross-peak volumes using the isolated two-spin approximation relationship, $r_{ij} = r_{kl} (\sigma_{kl}/\sigma_{ij})^{1/6}$, where σ_{ij} and σ_{kl} are the NOE intensities for the atom pairs i, j and k, l separated by distances r_{ij} and r_{kl} , respectively. A set of 42 distances were calculated and a restrained energy minimation were run using the Insight II/

Scheme 3. Synthesis of the Hexadecavalent Glycoclusters with RAFT Cyclopeptide Core (RD_{16} and RR_{16})^a

^aReagents and conditions: (a) 0.1% TFA in H₂O, 37 °C, 2 h, 65% for **9A**; 70% for **9B**; 77%³⁶ for **9C**; 89% for **11A**; 88% for **11B**; 82%³⁶ for **11C**. All amino acids belong to the L-series.

Discover software (Version 2005, Accelrys, San Diego, CA, USA). Calculations were performed in vacuo using the CVFF forcefield and a distance-dependent dielectric function of $\epsilon_r = 4r$. The starting structure was first subjected to 200 cycles of rEM with conjugate gradients. Then, molecular dynamic (MD) simulations were performed following the default protocol for simulated annealing starting at a temperature of 600 K slowly lowered to 300 K (time step = 1 fs, 8.6 ps MD, 500 conjugate-gradient minimization steps).⁴⁴

RESULTS AND DISCUSSION

Synthesis of Glycocyclopeptides. Fucosylated glycoclusters were synthesized following a highly efficient oxime conjugation protocol. This strategy required the preparation of aminoxy fucosyls that were obtained by treatment of fluoride donor **1**⁴⁵ with *N*-hydroxyphthalimide and BF₃·Et₂O. In order to evaluate the influence of the glycosidic linkage in the binding process with LecB, this glycosylation was performed in dichloromethane to afford both alpha (**2**) and beta anomers (**3**) that were easily separated by column chromatography (Scheme 1). Final deprotection with methylhydrazine provided pure derivatives **A** and **B** after recrystallization in ethanol. A similar procedure was employed to prepare aminoxy galactosyl **C**.⁴⁶

We next prepared several series of glycoclusters with diverse valency (i.e., 4, 6, and 16 carbohydrate units) and tridimensional architecture. Starting from the aldehyde-containing cyclopeptide scaffold **4** (R_4),³⁵ tetravalent glycoclusters **5A–C**

were synthesized by oxime condensation with sugar derivatives **A–C** in aqueous solution containing 0.1% of trifluoroacetic acid (TFA) (Scheme 2). For hexavalent glycoclusters, two lysines functionalized with serine were introduced on the second domain of the new cyclopeptide scaffold (R_6), providing two additional anchoring sites (**6**) after oxidative cleavage with sodium periodate (Scheme 2). Conjugation of sugars **A–C** under the same conditions afforded hexavalent derivatives **7A–C**.

We recently demonstrated that valency of glycocyclopeptides can be extended to sixteen sugar headgroups in a controlled manner using an iterative divergent protocol.³⁶ To this end lysine-based dendron and/or cyclopeptide functionalized with serines and an aminoxy linker were conjugated onto a cyclopeptide core such as **4**, then aldehydes were generated from serines to afford scaffolds **8** (RD_{16}) and **10** (RR_{16}). As shown previously with other sugars, attachment of aminoxy derivatives **A–C** occurred in short reaction time and mild acidic conditions to provide hexadecavalent glycoclusters **9A–C** and **11A–C** in excellent yields (Scheme 3).

By contrast with low molecular weight glycoclusters (i.e., **5A–C** and **7C**) which showed clear mass spectra by ESI, characterization of hexadecavalent glycoclusters by mass spectroscopy was delicate mainly due to the sensitivity of oxime linkage to fragmentations during the analysis. In addition we previously discovered that a careful precleaning protocol is a prerequisite to analyze these structures by mass.³⁶ By employing this sample preparation procedure we obtained in

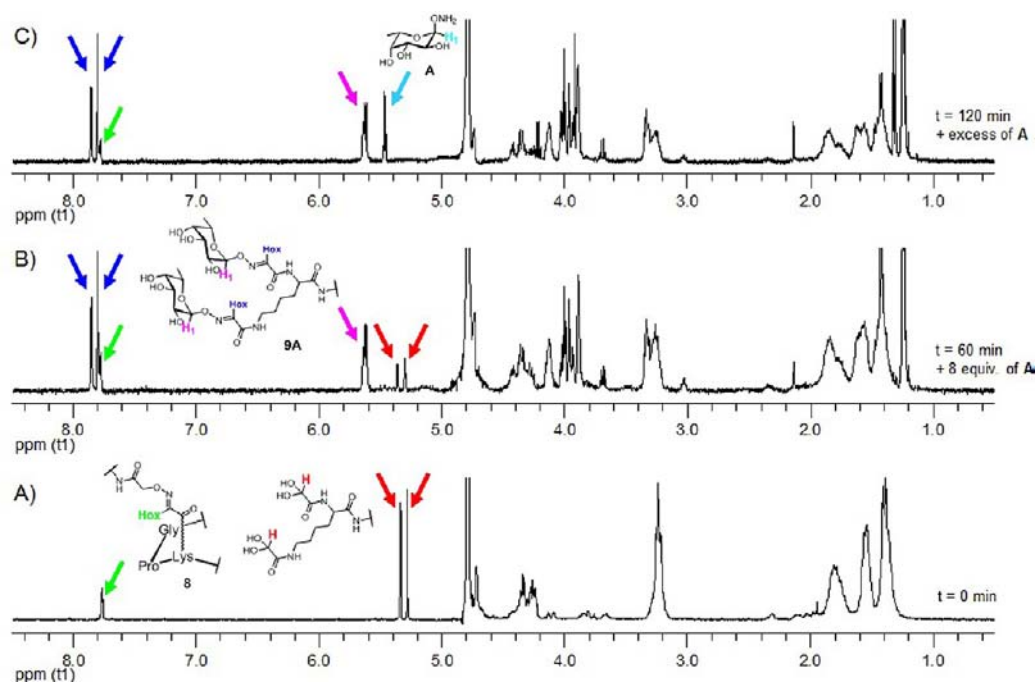


Figure 2. Oxime coupling between aldehyde-containing scaffold **8** and aminoxy α -fucosyl **A** monitored by ^1H NMR (400 MHz). (A) Scaffold **8** before addition of sugar **A** (red arrow: protons of the hydrated aldehydes; green arrow: oxime protons of the linkage between the cyclopeptide core and the lysine-based dendron). (B) Crude mixture after addition of 8 equiv of **A** and 1 h at 37 °C (purple arrow: anomeric protons of the linked sugars; blue arrow: oxime protons of the oxime linkage between the sugar and the peptide). (C) Crude mixture after addition of an excess of **A** and 1 h at 37 °C (cyan arrow: anomeric protons of unreacted sugar **A**).

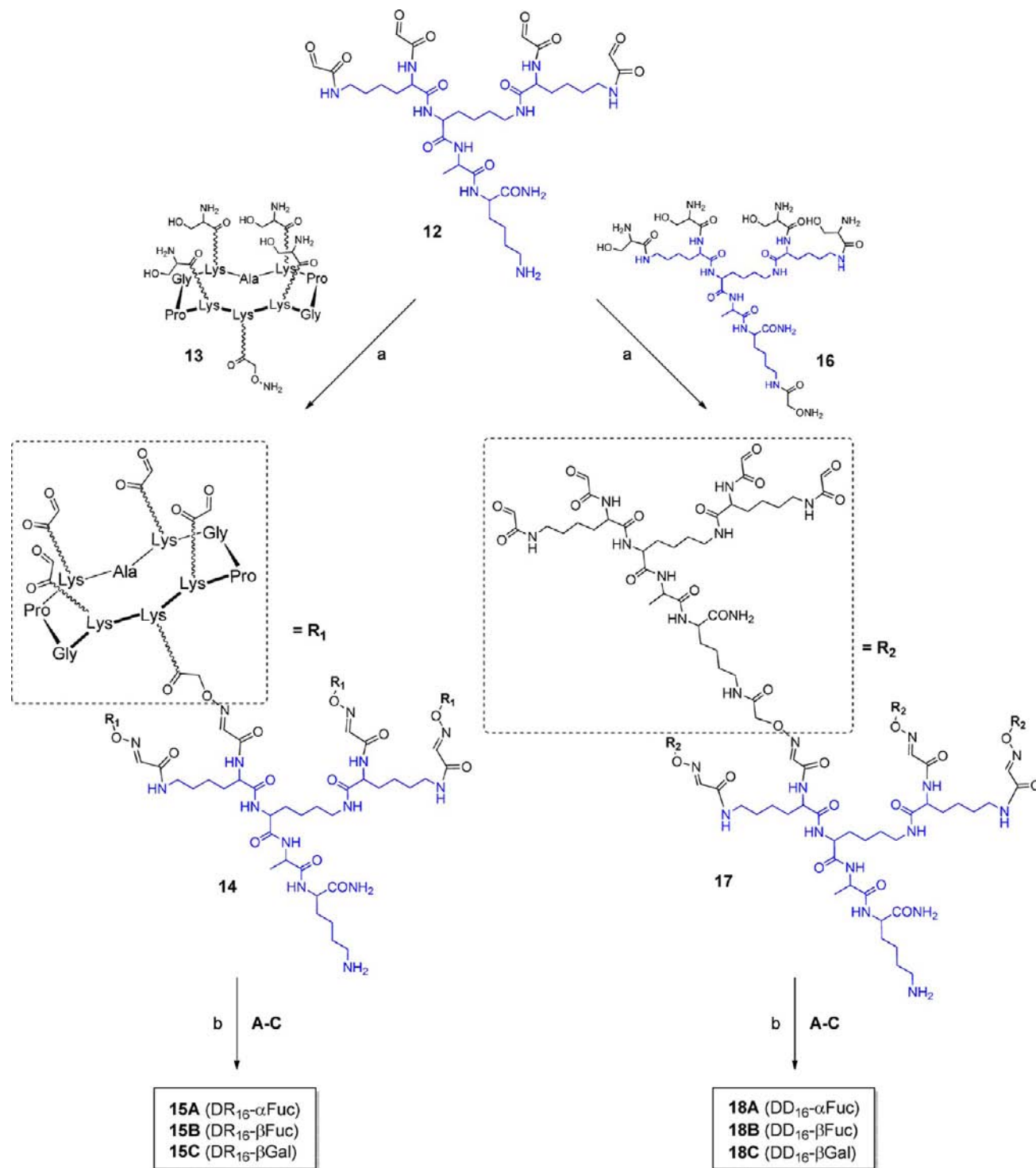
all cases MALDI-TOF spectra with the expected molecular peak (see Supporting Information), albeit showing a lot of signals which correspond to the oxime fragmentation rather than partially substituted structures. Interestingly, however, the final oxime coupling can be more easily followed by ^1H NMR to confirm the complete conversion and preclude the presence of partially glycosylated secondary structures. Reaction monitoring of the final oxime coupling (e.g., between scaffold **8** and aminoxy fucosyl **A** in D_2O containing 0.1% of TFA) is indicated in Figure 2. Despite the complexity of the NMR spectrum, two singulets corresponding to hydrated aldehydes (e.g., **8** linked to the $N\alpha$ and **8** to the side chain of lysine) were indeed observed at 5.28 and 5.34 ppm and the 4 oxime protons gave clear signals around 7.75 ppm with expected integration values (Figure 2A). After addition of 8 equiv of **A**, signals corresponding to anomeric protons of the linked fucose units and new oxime protons were clearly observed with concomitant decrease of hydrated aldehyde peaks. Total conversion of **8** was finally obtained by adding **A** in excess (i.e., 2 equiv per aldehyde) as proven by the complete disappearance of hydrated aldehyde and the presence of anomeric proton of unreacted sugar **A**, thus confirming the efficiency and completeness of the oxime conjugation procedure.

We employed a similar strategy to synthesize a new series of glycoclusters having a lysine-based dendron instead of a RAFT cyclopeptide core to provide more flexible frameworks (Scheme 4). In that case compound **12** was functionalized using 10-fold excess of RAFT cyclopeptide **13**⁴⁸ or dendrimer **16**⁴⁹ in 0.1% TFA in H_2O . Quantitative conversion of **12** was observed by HPLC analysis after 2 h. After quenching of unreacted **13** and **16** with acetone and subsequent treatment of the crude mixture with sodium periodate, aldehydic derivatives **14** (DR_{16}) and **17** (DD_{16}) were obtained in 30 min. Final

oxime coupling with aminoxy carbohydrates **A–C** under standard conditions provided hexadecavalent glycoclusters **15A–C** and **18A–C** after purification by preparative HPLC.

Enzyme-Linked Lectin Assays (ELLA). Binding properties of these glycoconjugates were studied toward LecB using ELLA. This experiment measure the ability of a ligand to inhibit the binding of lectins to immobilized poly[*N*-(2-hydroxyethyl)acrylamide] glycopolymers (PAA). With the lectin LecB, PAA- α -L-fucose was coated at the surface of microtiter plates and methyl α -L-fucopyranoside (α MeFuc) or methyl β -L-fucopyranoside (β MeFuc) were used as the monovalent reference for the α - and β -fucosylated glycoclusters, respectively.²¹ Results of ELLA inhibition tests are reported in Table 1.

α -Fucosylated Series. In the α -fucosylated series, tetravalent **5A** and hexavalent **7A** derivatives exhibited IC_{50} of 0.145 μM and 0.15 μM , respectively, which corresponds to a low improvement in comparison with α MeFuc (0.62 μM). When reported to the number of sugars, the value reaches 1, which denotes that inhibition is only due to a simple concentration effect instead of multivalency. More interestingly, stronger inhibition effects were obtained with the hexadecavalent clusters. In particular, while **11A**, **15A**, and **18A** showed IC_{50} at the same range of nanomolar concentrations (7.6 to 11 nM), compound **9A** provided the most significant effect with an IC_{50} measured at 0.6 nM, making this compound the best multivalent inhibitor reported for LecB. This value corresponds to a 1033-fold binding improvement (rp) in reference to α MeFuc, although its binding efficiency per sugar was rather moderate (rp/n of 65). We presume that this effect can be attributed in part to chelate binding mode, which is compatible with the size of the ligand and tridimensional features of LecB. In the meantime, this higher avidity might also be due to the formation of insoluble cross-linked complexes. It is worth

Scheme 4. Synthesis of the Hexadecavalent Glycoclusters with Dendrimer Core (DR₁₆ and DD₁₆)^a

^aReagents and conditions: (a) i: 0.1% TFA in H₂O, 37 °C, 2 h; ii: NaIO₄, H₂O, rt, 30 min, 78% for 14; 63% for 17; (b) 0.1% TFA in H₂O, 37 °C, 2 h, 66% for 15A; 75% for 15B; 73% for 15C; 73% for 18A; 70% for 18B; 65% for 18C. All amino acids belong to the L-series.

noting that glycoclusters presenting βGal units used as negative control did not reveal inhibition (at a maximum concentration of 200 μM for 9C, 11C, 15C, and 18C and 1 mM for 5C), thus confirming that inhibitory effects are due to the multiple presentation of fucose unit instead of secondary interactions with the peptidic skeleton.

β-Fucosylated Series. All the reported ligands for LecB display αFuc; however, the influence of the anomer

configuration to the binding was never investigated until now. Thus, we studied whether multivalent β-fucosylated derivatives can bind LecB even though βMeFuc (IC₅₀ of 70 μM) is more than 100-fold less active than αMeFuc. With tetravalent (5B) and hexavalent (7B) clusters, we observed an almost 20- and 60-fold increase of inhibitory potency relative to βMeFuc used as reference. On a per sugar basis, this represents however a modest 5- to 10-fold improvement. When the ligand valency

Table 1. ELLA Data for Glycoclusters with LecB Lectin

| compound | n^a | IC ₅₀ (nM) ^b | rp ^{c,d} | rp/ $n^{d,e}$ |
|----------------|-------|------------------------------------|-------------------|---------------|
| α MeFuc | 1 | 620 ± 30 | 1 | 1 |
| 5A | 4 | 145 ± 50 | 4.3 | 1 |
| 7A | 6 | 150 ± 30 | 4.1 | 0.7 |
| 9A | 16 | 0.6 ± 0.1 | 1033 | 64.6 |
| 11A | 16 | 11 ± 8 | 56.3 | 3.5 |
| 15A | 16 | 9.2 ± 1 | 67 | 4 |
| 18A | 16 | 7.6 ± 1 | 81 | 5 |
| β MeFuc | 1 | 70000 ± 11000 | 1 (0.009) | 1 (0.009) |
| 5B | 4 | 3790 ± 700 | 18.5 (0.16) | 4.6 (0.04) |
| 7B | 6 | 1250 ± 1000 | 56 (0.49) | 9.3 (0.08) |
| 9B | 16 | 109 ± 2 | 514 (5.68) | 40 (0.35) |
| 11B | 16 | 100 ± 80 | 680 (6.2) | 42 (0.38) |
| 15B | 16 | 51 ± 6 | 1372 (12.1) | 85.8 (0.76) |
| 18B | 16 | 71 ± 9 | 986 (8.7) | 61.6 (0.54) |

^aNumber of sugars in the cluster. ^bAverage of three independent experiments. ^cRelative potency "rp" = IC₅₀(monosaccharide)/IC₅₀(glycocluster). ^dValues in parentheses are expressed relative to the monomer α MeFuc. ^eRelative potency/sugar "rp/ n " = relative potency/ n .

increases, tremendous inhibitory effects were achieved for compounds **9B** (IC₅₀ of 109 nM) and **11B** (IC₅₀ of 100 nM) containing the cyclopeptide core. Even more remarkable results were observed with lysine-based dendritic structures since **15B** and **18B** gave IC₅₀ of 71 and 51 nM, respectively. For the best ligand of this series (i.e., **15B**), we indeed measured a relative potency of almost 1400 over β MeFuc. These data demonstrate that glycoclusters presenting fucosyls with beta anomeric linkage were good ligands for LecB as well, albeit being less active than the corresponding ligands of the α Fuc series.

Lectin Specificity and Scaffold Architecture. We next studied the selectivity of LecB for α -fucosylated glycoclusters, in comparison with their β -fucosylated analogues. Figure 3A first shows that β MeFuc is 113 times less active than α MeFuc by ELLA. This is in agreement with the well-known selectivity of LecB for α -fucosylated ligands since tridimensional studies did not reveal contact between the anomeric oxygen and the protein. However, we found a 182-fold amplification of selectivity for α -fucose with the scaffold **9** (IC₅₀(**9B**)/IC₅₀(**9A**) = 181.7) while the other scaffolds **5**, **7**, **11**, **15**, and **18** lead to a significant 26- to 5-fold decrease of selectivity in favor to β . This interesting data reflects a more favorable spatial orientation of sugar units in **9A** than in other clusters. We also studied how the cluster architecture in both series of

compounds influences the binding efficiency per sugar. Figure 3B clearly indicates that binding properties of β -fucosylated clusters systematically increase with the ligand valency, while significant improvements were achieved with a single hexadecavalent cluster (**9A**) in the alpha series. Minor differences were indeed observed with tetravalent (**5**) and hexavalent (**7**) scaffolds since the binding improvement was below 10. With hexadecavalent structures, the rigid cyclopeptide core functionalized with flexible lysine-based dendron (i.e., scaffold **9**) appeared to be the best scaffold to enhance the binding potency of α Fuc (rp/ n of 65), and β Fuc in a less extend (rp/ n of 40). On the other hand, hexadecavalent structures **11**, **15**, and **18** improved the binding of β Fuc much more efficiently than α Fuc. In particular, the best scaffolds for β Fuc was those with the flexible lysine-based core branched with conformationally constrained cyclopeptides (**15**) or lysine-based dendron (**18**) which both display sugar units with orientation allowing multivalent binding. All these results show that the binding properties of glycoclusters are strongly dependent on structural parameters that are orientation and distribution of the sugar units; size and nature of the spacer; and geometry and rigidity of the scaffold. In the present case, **9** and **15** are the more appropriate scaffolds to ensure multivalent binding of α Fuc and β Fuc, respectively.

Isothermal Titration Calorimetry (ITC). The compounds presenting the highest affinity for LecB and presenting α Fuc (**9A**) and β Fuc (**15B**) were used for titration microcalorimetry in order to determine the stoichiometry and thermodynamic contribution of the binding in solution. Compound **9B**, that carries β Fuc, was also tested in order to have a direct comparison with **9A** that has the same scaffold. Attempts to perform the titration in direct injection mode (i.e., ligand in syringe and protein in cell) resulted in too-rapid aggregation with unrelevant stoichiometry values. The reverse titration mode was previously proposed to be more suited for multivalent compounds⁵⁰ and gave better results here. Some aggregation was still observed but only after the titration stage. Typical thermograms obtained with the three compounds are displayed in Figure 4. Stoichiometry data indicate that each cluster can bind between 3 and 6 monomers of lectins, indicating that only some of the 16 fucose residues of each glycocluster can reach a lectin binding site. All three compounds displayed submicromolar affinities. The best ligand is compound **9A** (K_d = 28 nM), while the β Fuc containing ligand display K_d values 10 times higher. The fucose in the alpha anomeric state seems to be better presented for entering

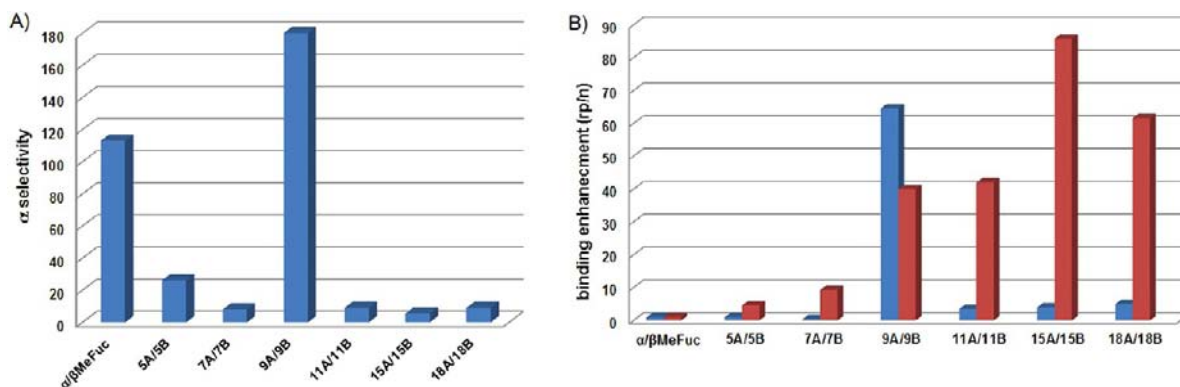


Figure 3. Comparison of (A) the selectivity for α Fuc; (B) the binding efficiency to LecB.

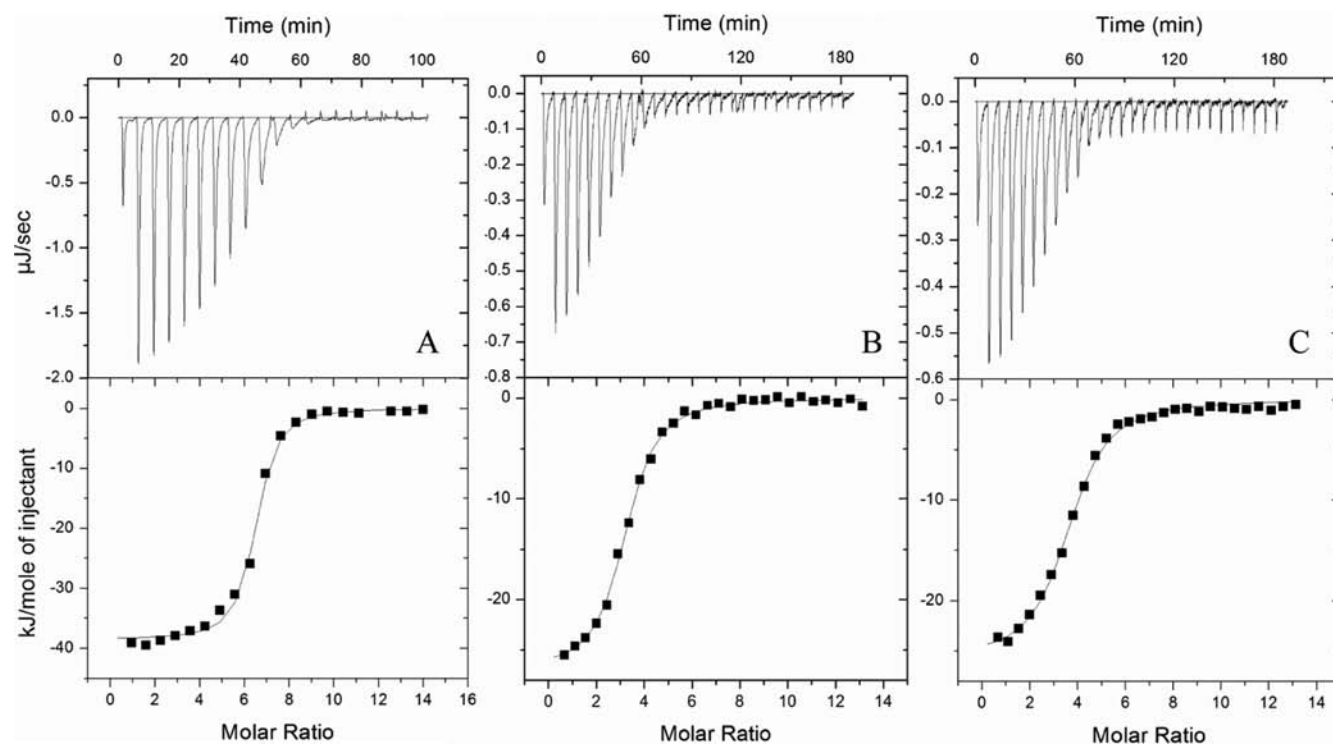


Figure 4. ITC data. Top: thermograms obtained by injections of lectin LecB (0.25 mM) in solution of compounds **9A** (A), **9B** (right), and **15B** (C) at 4 μ M. Bottom: corresponding integrated titration curves. Molar ratio is indicated as number of lectin monomers per glycocluster molecules.

Table 2. Isothermal Titration Microcalorimetry Data for Glycoconjugates Binding to LecB^a

| compound | K_d [nM] | $-\Delta H^\circ$ [kJ.mol ⁻¹] | $-T\Delta S^\circ$ [kJ.mol ⁻¹] | $-\Delta G^\circ$ [kJ.mol ⁻¹] | n |
|-----------------------------|--------------|---|--|---|-----------------|
| α MeFuc ^b | 430 \pm 10 | 41 \pm 1 | -5 | 36.4 | 0.77 \pm 0.03 |
| 9A | 28 \pm 6 | 222.8 \pm 3.6 | 179 | 43.1 | 0.19 \pm 0.02 |
| 9B | 213 \pm 21 | 85.5 \pm 0.2 | 47 | 38.1 | 0.30 \pm 0.01 |
| 15B | 307 \pm 75 | 82 \pm 10 | 45 | 37.2 | 0.29 \pm 0.02 |

^aThermodynamic data are referred to moles of glycoclusters and stoichiometry expressed as the number of glycocluster molecules per lectin monomer. Standard deviations have been estimated from at least two independent experiments (deviations on calculated $T\Delta S$ are similar to those on experimental ΔH). ^bFrom titration of α MeFuc in LecB in ref 20.

binding site as indicated by the stoichiometry, and also the shapes of the peaks. The very slow return to baseline observed for **9B** and **15B** indicates local rearrangement required for binding.

Analysis of the thermodynamic contributions (Table 2) indicates that for the three glycoclusters the binding is driven by enthalpy with significant entropy barrier observed in all cases. The higher affinity of compound **9A** results mainly from its very strong enthalpy of binding ($\Delta H^\circ = -223$ kcal/mol) indicating that α -fucosides fit better in the lectin binding site. This strong enthalpy term is however counterbalanced by a strong entropy term resulting from the limitation of conformation freedom upon lectin binding. Interestingly compounds **9B** and **15B** that are built on different scaffolds do not display significant differences in term of entropy of binding, therefore indicating a limited influence of their scaffold's geometry on the binding properties toward LecB. Assignment of nearly all protons was realized in a sequential manner using NOESY, DQFCOSY, and TOCSY spectra following the well-established strategy described for peptides.⁵¹ NMR data clearly indicate that this compound possesses a fourfold rotational pseudosymmetry leading to an equivalent magnetic environment for symmetry-related protons and,

therefore, a dramatic degeneration of chemical shifts (Figure 5). Hence, only one strand was observable. Nonpeptidic amide bonds, e.g., between two lysines *via* an oxime linker, were confirmed by observing NOE correlations from the NH ξ proton of the lysine side chain and the N=CH or the CH₂O protons of the oxime bond.

Molecular Modeling of Compound **9A**.

¹H NMR Resonance Assignments. Complete multidimensional NMR studies were carried out on the best inhibitor **9A** and assigned resonances are reported in Table 3.

Structural Calculations. Molecular modeling studies were conducted to further interpret the NMR data. Despite resonance degeneration due to symmetry it was possible to determine the spatial arrangement of one strand. For instance, distance constraints were unambiguously determined between two lysines linked by their side chains, thus allowing correct orientation of the oxime bond. A total of 42 NOE distances were measured and used as constraints for molecular modeling calculations. The four arms of glycocluster **9A** were built in a fully extended conformation with the Biopolymer module of Insight II/Discover software and attached to the cyclodecapeptide scaffold. This starting structure was first subjected to 200 cycles of restrained energy minimization (rEM) and

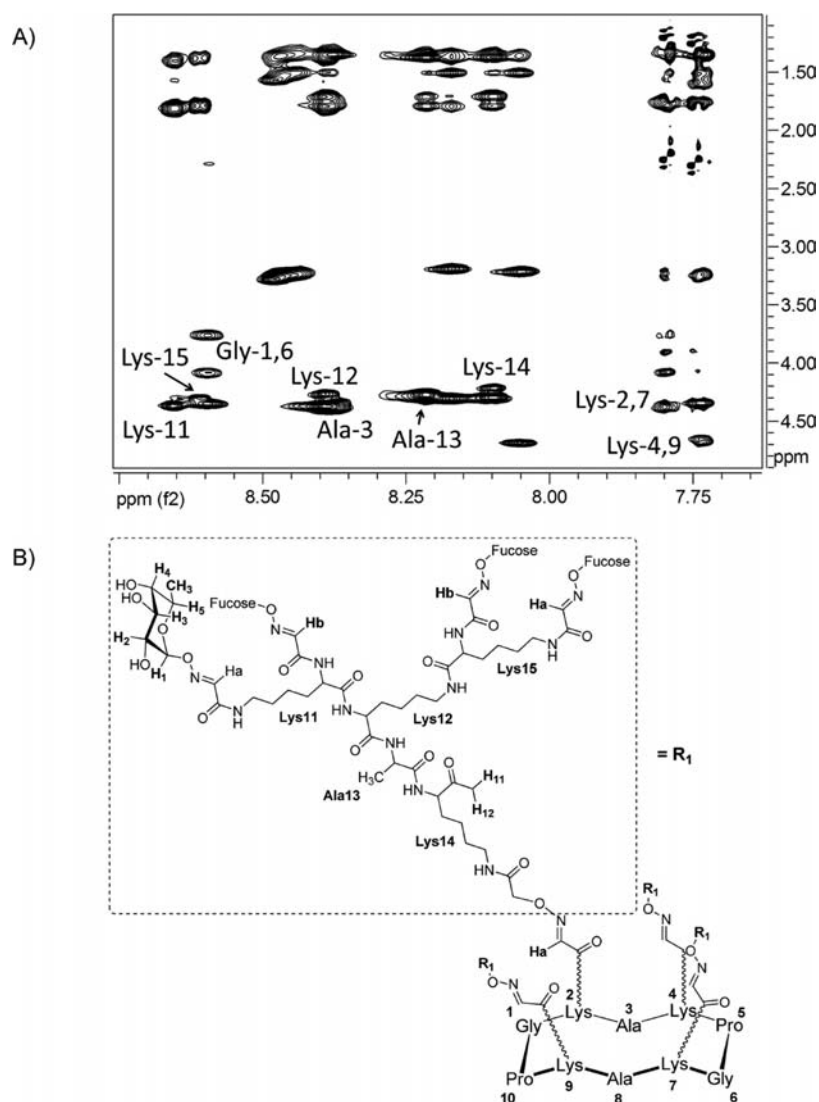


Figure 5. Expanded regions of a NOESY spectrum at 500 MHz in 95% H₂O/5% D₂O showing: (A) NH- α and NH-side chain correlations; (B) chemical structure and numbering scheme of **9A**.

Table 3. Proton Chemical Shift Assignments for Compound **9A in H₂O at 25°C**

| residue | HN | H α | H β | H γ | others |
|-----------------------|------------|------------|------------|------------|---|
| Gly-1/6 | 8.63 | 3.79, 4.11 | | | |
| Pro-5,10 | | 4.38 | 1.93, 2.32 | 2.08, 2.02 | CH ₂ δ 3.85, 3.66 |
| Lys-2,7 | 7.83 | 4.41 | 1.80 | 1.36 | CH ₂ δ 1.55; CH ₂ ϵ 3.25; NH 8.46 |
| Ala-3,8 | 8.40 | 4.38 | 1.37 | | |
| Lys-4,9 | 7.77 | 4.69 | 1.78, 1.64 | 1.37 | CH ₂ δ 1.55; CH ₂ ϵ 3.32; NH 8.47 |
| Lys-11 | 8.69 | 4.40 | 1.84 | 1.40 | CH ₂ δ 1.59; CH ₂ ϵ 3.31; NH 8.51 |
| Lys-12 | 8.42 | 4.30 | 1.83, 1.73 | 1.38 | CH ₂ δ 1.53; CH ₂ ϵ 3.23; NH 8.08 |
| Ala-13 | 8.25 | 4.33 | 1.40 | | |
| Lys-14 | 8.13 | 4.24 | 1.82, 1.73 | 1.37 | CH ₂ δ 1.54; CH ₂ ϵ 3.22; NH 8.20 |
| Lys-15 | 8.64 | 4.34 | 1.82 | 1.38 | CH ₂ δ 1.57; CH ₂ ϵ 3.27; NH 8.47 |
| N=CH-ox | 7.82, 7.76 | | | | |
| CH ₂ -O-ox | 4.70 | | | | |
| Fucose | 5.61 (H1) | 3.99 (H2) | 3.86 (H3) | 4.02 (H4) | 1.21 (CH ₃) |

followed by a high-temperature simulated annealing protocol for restrained molecular dynamics (rMD) simulations. Calculations were performed *in vacuo*, and the energy of the system was calculated by the consistent CVFF force field. The last 10 coordinate sets of the rMD protocol were averaged and

subjected to a final 500 steps of rEM to generate the restrained structure presented in Figure 6.

Interaction with LecB. To rationalize ITC data and evaluate the capacity of **9A** to bind several units of LecB, we performed a molecular modeling study. Starting from the structure

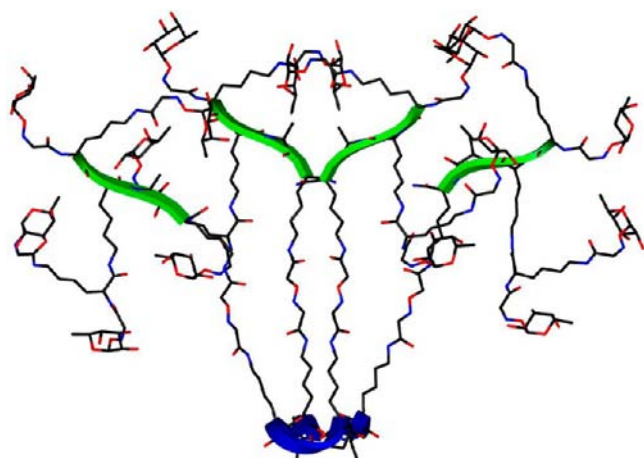


Figure 6. NMR-restrained MD model of the glycocluster **9A**. The cyclodecapeptide is represented as a blue ribbon and lysine-based dendrons are highlighted with green ribbons.

previously obtained (Figure 6), the four longest arms were spread out to a distance between each fucose unit of approximately 50 Å. The fucose residues were given in ${}^1\text{C}_4$ conformation similar to that observed in the crystal structure in complex with L-fucose (pdb 1GZT), which corresponds to the most stable conformation upon binding.¹⁸ The complex between two LecB tetramers and **9A** was constructed by docking the fucose into the cavity in the position it occupies in the crystallographic structure with proper coordination with two calcium ions. Intermolecular distance restraints were added to maintain the fucose in the correct position and the complex was subjected to energy minimizations and restrained molecular dynamics (rMD). Finally, the structure was released from all constraints and subsequently energy minimized. We obtained a model (Figure 7) showing that the glycodendrimer **9A** can easily accommodate four monomers and no steric clashes were

encountered, which is in agreement with the stoichiometry measured by ITC. We anticipated that it would be possible to bind at least one more monomer in each side of the glycocluster since the four remaining lateral arms are flexible and long enough to interact with LecB without generating steric conflict.

CONCLUSION

In summary, cyclopeptide and lysine-based dendron were conjugated in all possible arrangements using an iterative oxime ligation procedure. Their final functionalization with α Fuc and β Fuc provided a new series of hexadecaivalent glycosylated scaffolds with different architecture and flexibility that were tested with the lectin LecB from *Pseudomonas aeruginosa* in competitive ELLA tests. We first observed that tetraivalent and hexavalent presentation of both anomers of fucose (**5A–C** and **7A–C**) did not ensure significant binding enhancement to LecB. However, the hexadecaivalent systems displaying α Fuc resulted in IC_{50} in the nanomolar range, whereas derivative **9A** (RD architecture) gave the strongest binding improvement (IC_{50} of 0.6 nM) over α MeFuc with an increase of α -selectivity of LecB. ITC experiments confirmed the binding ability of **9A** which has the highest affinity (K_d of 28 nM) ever reported for LecB, and a stoichiometry of binding indicating up to six monomers of lectin per glycodendrimer. A molecular model of **9A** interacting with two lectin tetramers was thus proposed to rationalize these experimental data and suggested that high affinity might due to an aggregative chelate binding mode. By contrast, even though β -fucosylated structures are typically low affinity ligands of LecB (IC_{50} of 70 μM for β MeFuc), hexadecaivalent derivatives in the β series showed unprecedented activity (IC_{50} from 51 to 109 nM) albeit showing a slight difference of inhibitory effect in favor of the more flexible lysine-based dendritic structures (**15B** and **18B**). Altogether, these results highlight the influence of the ligand valency, the architecture, and the anomer configuration for binding to LecB

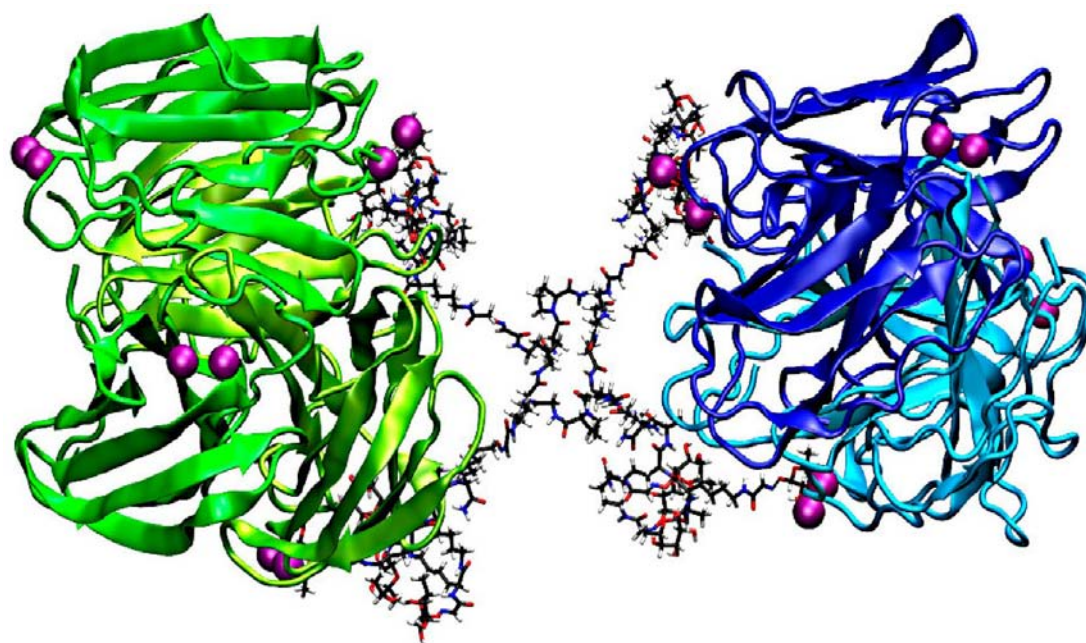


Figure 7. Molecular modeling-based structure of the LecB-**9A** complex. The protein is shown as ribbons, the glycocluster is represented as sticks, and the calcium ions as purple spheres.

and suggest that even low affinity ligands displayed by multivalent scaffolds can reach high affinity. These promising results together with the stability of oxime linkage both *in vitro* and *in vivo*⁵² prompt us to further investigate the effect of our structures, in particular on the *P. aeruginosa* biofilm formation or dispersion.

■ ASSOCIATED CONTENT

■ Supporting Information

Additional spectra and characterization data. This material is available free of charge via the Internet at <http://pubs.acs.org>.

■ AUTHOR INFORMATION

Corresponding Author

*E-mail: olivier.renaudet@ujf-grenoble.fr.

Notes

The authors declare no competing financial interest.

■ ACKNOWLEDGMENTS

This work was supported by the Université Joseph Fourier (UJF), the Centre National de la Recherche Scientifique (CNRS), the “Communauté d’agglomération Grenoble-Alpes Métropole” (Nanobio Program), and the “Communautés de Recherche Académique Rhône Alpes (ARC-1)”. A.I. and O.R. acknowledge support from the Labex Arcane (ANR-11-LABX-003) and the COST action CM1102. A.I. is also grateful for support from GDR *Pseudomonas* and COST action BM1003. O.R. gratefully acknowledge the ANR-12-JS07-0001-01 “Vac-Syn”.

■ REFERENCES

- (1) Varki, A. (1993) Biological roles of oligosaccharides: all of the theories are correct. *Glycobiology* 3, 97–130.
- (2) Dwek, R. A. (1996) Glycobiology: toward understanding the function of sugars. *Chem. Rev.* 96, 683–720.
- (3) Lis, H., and Sharon, N. (1998) Lectins: carbohydrate-specific proteins that mediate cellular recognition. *Chem. Rev.* 98, 637–674.
- (4) Bertozzi, C. R., and Kiessling, L. L. (2001) Chemical glycobiology. *Science* 291, 2357–2364.
- (5) Sharon, N. (1996) Carbohydrate-lectin interactions in infectious disease. *Adv. Exp. Med. Biol.* 408, 1–8.
- (6) Imberty, A., and Varrot, A. (2008) Microbial recognition of human cell surface glycoconjugates. *Curr. Opin. Struct. Biol.* 18, 567–576.
- (7) Pieters, R. J. (2011) Carbohydrate mediated bacterial adhesion. *Adv. Exp. Med. Biol.* 715, 227–240.
- (8) Gilboa-Garber, N. (1982) *Pseudomonas aeruginosa* lectins. *Methods Enzymol.* 83, 378–385.
- (9) Imberty, A., Wimmerova, M., Mitchell, E. P., and Gilboa-Garber, N. (2004) Structures of the lectins from *Pseudomonas aeruginosa*: insights into the molecular basis for host glycan recognition. *Microb. Infect.* 6, 221–228.
- (10) Bernardi, A., Jiménez-Barbero, J., Casnati, A., De Castro, C., Darbre, T., Fieschi, F., Finne, J., Funken, H., Jaeger, K.-E., Lahmann, M., Lindhorst, T. K., Marradi, M., Messner, P., Molinaro, A., Murphy, P. V., Nativi, C., Oscarson, S., Penadés, S., Peri, F., Pieters, R. J., Renaudet, O., Reymond, J.-L., Richichi, B., Rojo, J., Sansone, F., Schäffer, C., Turnbull, W. B., Velasco-Torrijos, T., Vidal, S., Vincent, S., Wennekes, T., Zuilhof, H., and Imberty, A. (2013) Multivalent glycoconjugates as anti-pathogenic agents. *Chem. Soc. Rev.* 42, 4709–4727.
- (11) Imberty, A., Chabre, Y. M., and Roy, R. (2008) Glycomimetics and glycodendrimers as high affinity microbial anti-adhesins. *Chem.—Eur. J.* 14, 7490–7499.

- (12) Branson, T. R., and Turnbull, W. B. (2013) Bacterial toxin inhibitors based on multivalent scaffolds. *Chem. Soc. Rev.* 42, 4613–4622.

- (13) Chemani, C., Imberty, A., de Bentzmann, S., Pierre, M., Wimmerova, M., Guery, B. P., and Faure, K. (2009) Role of LecA and LecB lectins in *Pseudomonas aeruginosa*-induced lung injury and effect of carbohydrate ligands. *Infect. Immun.* 77, 2065–2075.

- (14) Hauber, H. P., Schulz, M., Pforte, A., Mack, D., Zabel, P., and Schumacher, U. (2008) Inhalation with fucose and galactose for treatment of *Pseudomonas aeruginosa* in cystic fibrosis patients. *Int. J. Med. Sci.* 5, 371–376.

- (15) Lee, Y. C., and Lee, R. T. (1995) Carbohydrate-protein interactions: basis of glycobiology. *Acc. Chem. Res.* 28, 321–327.

- (16) Mammen, M., Choi, S. K., and Whitesides, G. M. (1998) Polyvalent interactions in biological systems: implications for design and use of multivalent ligands and inhibitors. *Angew. Chem., Int. Ed.* 37, 2755–2794.

- (17) Lundquist, J. J., and Toone, E. J. (2002) The cluster glycoside effect. *Chem. Rev.* 102, 555–578.

- (18) Mitchell, E., Houles, C., Sudakevitz, D., Wimmerova, M., Gautier, C., Pérez, S., Wu, A. M., Gilboa-Garber, N., and Imberty, A. (2002) Structural basis for oligosaccharide-mediated adhesion of *Pseudomonas aeruginosa* in the lungs of cystic fibrosis patients. *Nat. Struct. Biol.* 9, 918–921.

- (19) Perret, S., Sabin, C., Dumon, C., Pokorna, M., Gautier, C., Galanina, O., Ilija, S., Bovin, N., Nicaise, M., Desmadril, M., Gilboa-Garber, N., Wimmerova, M., Mitchell, E. P., and Imberty, A. (2005) Structural basis for the interaction between human milk oligosaccharides and the bacterial lectin PA-IIL of *Pseudomonas aeruginosa*. *Biochem. J.* 389, 325–332.

- (20) Sabin, C., Mitchell, E. P., Pokorna, M., Gautier, C., Utille, J.-P., Wimmerova, M., and Imberty, A. (2006) Binding of different monosaccharides by lectin PA-IIL from *Pseudomonas aeruginosa*: thermodynamics data correlated with X-ray structures. *FEBS Lett.* 580, 982–987.

- (21) Marotte, K., Preville, C., Sabin, C., Moume-Pymbock, M., Imberty, A., and Roy, R. (2007) Synthesis and binding properties of divalent and trivalent clusters of the Lewis a disaccharide moiety to *Pseudomonas aeruginosa* lectin PA-IIL. *Org. Biomol. Chem.* 5, 2953–2961.

- (22) Andreini, M., Anderlüh, M., Audfray, A., Bernardi, A., and Imberty, A. (2010) Monovalent and bivalent *N*-fucosyl amides as high affinity ligands for *Pseudomonas aeruginosa* PA-IIL lectin. *Carbohydr. Res.* 345, 1400–1407.

- (23) Deguise, I., Lagnoux, D., and Roy, R. (2007) Synthesis of glycodendrimers containing both fucoside and galactoside residues and their binding properties to PA-IL and PA-IIL lectins from *Pseudomonas aeruginosa*. *New J. Chem.* 31, 1321–1331.

- (24) Marotte, K., Sabin, C., Prévaille, C., Moumé-Pymbock, M., Wimmerova, M., Mitchell, E. P., Imberty, A., and Roy, R. (2007) X-ray structures and thermodynamics of the interaction of PA-IIL from *Pseudomonas aeruginosa* with disaccharide derivatives. *ChemMedChem* 2, 1328–1338.

- (25) Morvan, F., Meyer, A., Jochum, A., Sabin, C., Chevolut, Y., Imberty, A., Praly, J.-P., Vasseur, J.-J., Souteyrand, E., and Vidal, S. (2007) Fucosylated pentaerythrityl phosphodiester oligomers (PePOs): automated synthesis of DNA-based glycoclusters and binding to *Pseudomonas aeruginosa* lectin (PA-IIL). *Bioconjugate Chem.* 18, 1637–1643.

- (26) Reymond, J.-L., Bergmann, M., and Dabre, T. (2013) Glycopeptide dendrimers as *Pseudomonas aeruginosa* biofilm inhibitors. *Chem. Soc. Rev.* 42, 4814–4822.

- (27) Kolomiets, E., Johansson, E. M., Renaudet, O., Darbre, T., and Reymond, J.-L. (2007) Neoglycopeptide dendrimer libraries as a source of lectin binding ligands. *Org. Lett.* 9, 1465–1468.

- (28) Johansson, E. M. V., Cruz, S. A., Kolomiets, E., Buts, L., Kadam, R. U., Cacciarini, M., Bartels, K.-M., Diggie, S. P., Cámara, M., Williams, P., Loris, R., Nativi, C., Rosenau, F., Jaeger, K.-E., Darbre, T., and Reymond, J.-L. (2008) Inhibition and dispersion of *Pseudomonas*

aeruginosa biofilms by glycopeptide dendrimers targeting the fucose-specific lectin LecB. *Chem. Biol.* 15, 1249–1257.

(29) Kolomiets, E., Swiderska, M. A., Kadam, R. U., Johansson, E. M. V., Jaeger, K.-E., Darbre, T., and Reymond, J.-L. (2009) Glycopeptide dendrimers with high affinity for the fucose-binding lectin LecB from *Pseudomonas aeruginosa*. *ChemMedChem* 4, 562–469.

(30) Johansson, E. M. V., Kadam, R. U., Rispoli, G., Crusz, S. A., Bartels, K.-M., Diggle, S. P., Camara, M., Williams, P., Jaeger, K.-E., Darbre, T., and Reymond, J.-L. (2011) Inhibition of *Pseudomonas aeruginosa* biofilms with a glycopeptide dendrimer containing D-amino acids. *MedChemComm* 2, 418–420.

(31) Galan, M. C., Dumy, P., and Renaudet, O. (2013) Multivalent glycol(cyclo)peptides. *Chem. Soc. Rev.* 42, 4599–4612.

(32) Renaudet, O., BenMohamed, L., Dasgupta, G., Bettahi, I., and Dumy, P. (2008) Towards self-adjuvanting multivalent B and T-cell epitopes synthetic glyco-lipopeptide cancer vaccine. *ChemMedChem* 3, 737–741.

(33) Renaudet, O., Dasgupta, G., Bettahi, I., Shi, A., Nesburn, A. B., Dumy, P., and BenMohamed, L. (2010) Linear and branched glycolipopeptides vaccines follow distinct cross-presentation pathways and generate different magnitudes of antitumor immunity. *Plos ONE* 5, e11216.

(34) Pujol, A. M., Cuillel, M., Renaudet, O., Lebrun, C., Charbonnier, P., Cassio, D., Gateau, C., Dumy, P., Mintz, E., and Delangle, P. (2011) Hepatocyte targeting and intracellular copper chelation by a thiol-containing glycocyclopeptide. *J. Am. Chem. Soc.* 133, 286–296.

(35) Renaudet, O., and Dumy, P. (2003) Chemoselectively template-assembled glycoconjugates as mimics for multivalent presentation of carbohydrates. *Org. Lett.* 5, 243–245.

(36) Bossu, I., Šulc, M., Křenek, K., Dufour, E., Garcia, J., Berthet, N., Dumy, P., Křen, V., and Renaudet, O. (2011) Dendri-RAFTs: a second generation of cyclopeptide-based glycoclusters. *Org. Biomol. Chem.* 9, 1948–1959.

(37) André, S., Renaudet, O., Bossu, I., Dumy, P., and Gabius, H.-J. (2011) Cyclic glycodecapeptides: how to increase their inhibitory activity and selectivity on lectin/toxin binding to a glycoprotein and cells. *J. Pept. Sci.* 17, 427–437.

(38) Mitchell, E. P., Sabin, C., Snajdrova, L., Budova, M., Perret, S., Gautier, C., Hofr, C., Gilboa-Garber, N., Koča, J., Wimmerová, M., and Imberty, A. (2005) High affinity fucose binding of *Pseudomonas aeruginosa* lectin PA-III: 1.0 Å resolution crystal structure of the complex combined with thermodynamics and computational chemistry approaches. *Proteins: Struct. Funct. Bioinf.* 58, 735–746.

(39) Braunschweiler, L., and Ernst, R. R. (1983) Heteronuclear correlation spectroscopy in rotating solids. *J. Magn. Reson.* 53, 521–528.

(40) Piantini, U., Sørensen, O. W., and Ernst, R. R. (1982) Multiple quantum filters for elucidating NMR coupling networks. *J. Am. Chem. Soc.* 104, 6800–6801.

(41) Jeener, J., Meier, B. H., Bachmann, P., and Ernst, R. R. (1979) Investigation of exchange processes by 2-dimensional NMR-spectroscopy. *J. Chem. Phys.* 71, 4546–4553.

(42) Shaka, A. J., Lee, C. J., and Pines, A. (1988) Iterative schemes for bilinear operators - application to spin decoupling. *J. Magn. Reson.* 77, 274–293.

(43) Hwang, T. L., and Shaka, A. J. (1995) Water suppression that works - excitation sculpting using arbitrary wave-forms and pulsed-field gradients. *J. Magn. Reson.* 112, 275–279.

(44) Dayringer, H. E., Tramontano, A., Sprang, S. R., and Fletterick, R. J. (1986) Interactive program for visualization and modeling of proteins, nucleic-acids and small molecules. *J. Mol. Graph.* 6, 82–87.

(45) Duléry, V., Renaudet, O., Philouze, C., and Dumy, P. (2007) α or β L-fucopyranosyl oxyamines: key intermediates for the preparation of fucose-containing glycoconjugates by oxime ligation. *Carbohydr. Res.* 342, 894–900.

(46) Renaudet, O., and Dumy, P. (2001) Expedient synthesis of aminoxyated-carbohydrates for chemoselective access of glycoconjugates. *Tetrahedron Lett.* 42, 7575–7578.

(47) Bossu, I., Berthet, N., Dumy, P., and Renaudet, O. (2011) Synthesis of glycocyclopeptides by click chemistry and inhibition assays with lectins. *J. Carbohydr. Chem.* 30, 458–468.

(48) Grigalevicius, S., Chierici, S., Renaudet, O., Lo-Man, R., Dériaud, E., Leclerc, C., and Dumy, P. (2005) Chemoselective assembly and immunological evaluation of multiepitopic glycoconjugates bearing clustered Tn antigen as synthetic anticancer vaccine. *Bioconjugate Chem.* 5, 1149–1159.

(49) Duléry, V., Renaudet, O., and Dumy, P. (2007) Ethoxyethylidene protecting group prevents N-overacylation in aminoxy peptide synthesis. *Tetrahedron* 63, 11952–11958.

(50) Dam, T. K., Roy, R., Pagé, D., and Brewer, C. F. (2002) Thermodynamic binding parameters of individual epitopes of multivalent carbohydrates to Concanavalin A as determined by “reverse” Isothermal Titration Microcalorimetry. *Biochemistry* 41, 1359–1363.

(51) Wüthrich, K. (1986) *NMR of Proteins and Nucleic Acids*, John Wiley and Sons, New York.

(52) Nardin, E. H., Calvo-Calle, J. M., Oliveira, G. A., Clavijo, P., Nussenzweig, R., Simon, R., Zeng, W., and Rose, K. (1998) Plasmodium falciparum polyoximes: highly immunogenic synthetic vaccines constructed by chemoselective ligation of repeat B-cell epitopes and a universal T-cell epitope of CS protein. *Vaccine* 16, 590–600.